Discovery and Significance of High CH$_4$ Primary Fluid Inclusions in Reservoir Volcanic Rocks of the Songliao Basin, NE China

WANG Pujun[1, *], HOU Qijun[2], WANG Keyong[1], CHEN Shumin[3], CHENG Rihui[1], LIU Wanzhu[1] and LI Quanlin[1]

1 *Earth Sciences College, Jilin University, Changchun, Jilin 130061*
2 *Jilin Petroleum Company, Songyuan, Jilin 138000*
3 *Daqing Petroleum Company, Daqing, Heilongjiang 163712*

Abstract: Comparing compositions of the fluid inclusions in volcanic rocks to the contents and isotopes of the gases in corresponding volcanic reservoirs using microthermometry, Raman microspectroscopy and mass spectrum analysis, we found that: (1) up to 82 mole% methane exists in the primary inclusions hosted in the reservoir volcanic rocks; (2) high CH$_4$ inclusions recognized in the volcanic rocks correspond to CH$_4$-bearing CO$_2$ reservoirs that are rich in helium and with a high ^{3}He/^{4}He ratio and which show reversed order of δ^{13}C in alkane; (3) in gas reservoirs of such abiotic methane (>80%) and a mix of CH$_4$ and CO$_2$, the enclosed content of CH$_4$ in the volcanic inclusions is usually below 42 mole%, and the reversed order of δ^{13}C in alkane is sometimes irregular in the corresponding gas pools; (4) a glassy inclusion with a homogeneous temperature over 900°C also contains a small portion of CH$_4$ although predominantly CO$_2$. This affinity between gas pool and content of inclusion in the same volcanic reservoirs demonstrates that magma-originated gases, both CH$_4$ and CO$_2$, have contributed significantly to the corresponding gas pools and that the assumed hydrocarbon budget of the bulk earth might be much larger than conventionally supposed.

Key words: Songliao Basin, reservoir volcanic rocks, fluid inclusions, methane (CH$_4$), carbon dioxide (CO$_2$), abiogenic origin natural gas

1 Introduction

Abiotic methane has been proven in deep-seated fluid inclusions and can also be generated by several processes such as respeciation of magmatic volatiles (Kelley, 1996), the Fischer-Tropsch synthesis (Salvi and William-Jones, 1997), and geothermal sources (Sheppard, 1981). However, whether these abiogenic hydrocarbons have any commercial value is still in question. One case report is provided by natural gases commercially produced from volcanic rocks in northeastern Japan. Wakita and Sano (1983) claimed, based on ^{3}He/^{4}He measurement, that more than one-third of the total methane might have been derived from upper mantle magmatic activity. But Sakata et al. (1989) thought, based on geochemical analysis, that no more than 0.1% of the total methane can be attributed to a magmatic origin. A similar debate has also taken place for the Songliao Basin of NE China.

In recent years there has been burgeoning interest in and debate about the abiogenic methane accumulated in commercial quantities in the Mesozoic volcanic reservoirs of the Songliao Basin. People in favor of an inorganic origin for the natural gas (e.g. Guo et al., 1994, 1997) provided the following evidence: (1) reservoirs are controlled by deep-seated faults and show close affinity to volcanism; (2) the isotopically heavy CH$_4$ (δ^{13}C> −30‰) is similar to that typical of abiogenic methane enclosed in mantle-derived inclusions in the basalt of the region (Liu et al., 1998; Wang et al., 2000); (3) the isotopic composition of co-existing helium is ca. 3 times the R_a (where R_a denotes the atmospheric ^{3}He/^{4}He ratio of 1.39×10^{-6}), presenting a mantle-derived signature (Xu et al., 1995); (4) the reversed orders of δ^{13}C in alkane (δ^{13}C$_1$ > δ^{13}C$_2$ > δ^{13}C$_3$ > δ^{13}C$_4$) suggest abiogenic contributions (Dai et al., 2003). However, others have argued that methane-dominant (C$_1$/C$_{2\ 3}$>100) coal gas can also have δ^{13}C$_{CH4}$ values above −30‰ (Dai, 1993) and so noble gases like helium may not originate from the same source as that of the co-existing

Table 1 Analytical data for selected inclusions in quartz of the representative reservoir volcanic rocks of the Songliao Basin

Sample	FS9-2		FS9-1					ZS6-1					SHS2		SOS1		ZS5	SiS1	FS7
Inclusion No.	1	4*	0	1	2	3	4	1	2	3	4	6	1*	1	2*	3*	1*	1*	1*
Th (°C)	375		368	395	315	312	295	386	298	305	293	306		377					>900
Filling degree	0.1	0.0	0.1	0.5	0.7	0.7	0.7	0.3	0.7	0.7	0.7	0.6	0.0	0.3	0.0	0.0	0.0	0.0	0.7
Tm_{CO2} (°C)	−64.2	−69.2	−66.1	−63.5	−61.0	−66.5	−64.6	−62.7	−56.9	−57.2	−56.9	−56.9	−62.5	−62.8	−64.0	−59.7	−59.7	−63.2	−57.0
Th_{CO2} (°C)	−20.0	−45.2	−39.4	−4.3	7.2	−38.5	−30.2	−6.8	8.6	8.0	8.4	8.0	−8.3	−10.5	−12.3	4.8	5.2	−10.3	7.9
Tm_{clath} (°C)	13.9		14.8	12.1	10.9	14.8	13.6	12.9	8.2	8.1	8.4	8.3		13.2					
Salinity (%)	5.0±		5.0±	4.4±	4.0±	5.0±	4.9±	4.0±	5.0	4.4	4.6	4.7		4.8±					
Dv	0.64		0.53	0.54	0.73	0.45	0.63	0.61	0.75	0.69	0.72	0.70		0.75					
Dl	1.06		1.09	1.10	1.10	1.08	1.07	1.06	1.07	1.08	1.07	1.07		1.06					
Vapor phase (mole %) CH₄	40.5	82.5	66.1	29.0	16.8	61.9	49.9	27.9	3.7	3.9	1.0	2.5	34.2	30.7	43.4	16.6	14.8	31.8	2.7
Vapor phase (mole %) CO₂	59.5	17.5	33.9	71.0	83.2	38.1	50.1	72.1	96.3	96.1	99.0	97.5	65.8	69.3	56.6	83.4	85.2	68.2	97.3
Bulk comp. (%) CH₄	31.2	82.5	58.8	5.4	1.9	5.9	8.3	11.0	0.6	0.8	0.2	0.3	34.2	14.0	43.4	16.6	14.8	31.8	2.7
Bulk comp. (%) CO₂	52.0	17.5	25.6	15.3	11.3	5.7	4.5	29.5	14.5	17.7	16.2	19.5	65.8	37.6	56.6	83.4	85.2	68.2	97.3
Bulk comp. (%) H₂O	16.8		15.6	79.3	86.8	88.4	87.2	59.5	84.9	81.5	83.6	80.2		48.4					

Notes: (1) Samples with asterisk are monophase or melt inclusions; (2) symbols as in text, Th: temperature of total homogenization of the inclusion (°C); Tm_{CO2} (Tm_{clath}): melting temperature of solid CO_2 (clathrate) in the presence of vapor (°C); Th_{CO2}: homogenization temperature of the non-aqueous part (°C); Dl (Dv): density of the aqueous part (of the non-aqueous part) (g/cm³).

methane. In addition, the reversed orders of $\delta^{13}C$ in alkane can also be generated by such processes as mixing of genetically different gases, either by evolution of the source rocks themselves or by leaking fractionation within cap rocks (Zheng et al., 1999; Li et al., 1999; Huang, 2000).

Owing to the variety of source rocks and complex geological settings of the Songliao Basin (Wang et al., 1993), most of the reservoirs could be composed of mixed gases from different origins possibly including biodegraded alkanes (Wang et al., 2004). So the contribution of abiogenic alkane to the commercial gas pools is still uncertain. A key point to this problem is to provide direct evidence for abiogenic gases and to indicate their relationship with the commercial gases hosted in the reservoir. The purpose of this paper is to assess the contribution of abiotic methane to the commercial gas reservoirs in the Songliao Basin. Commercial natural gases trapped in volcanic reservoir constitute mobile gases in that they can migrate within the reservoir. In contrast with these exploitable gases, the fluids hosted in minerals of the volcanic rocks are restricted gases. We compare composition and isotopes between the two kinds of gases contained in the same volcanic rocks in order to find the relationship between them. And finally we hope to get a conclusive answer about whether or not these abiogenic gases have contributed significantly to the corresponding commercial gas pools.

2 Geological Setting and Sampling

Situated in the northeast (Fig. 1), the Songliao Basin is the most important oil and gas-bearing basin in China owing to its annual crude oil equivalent production of over 50 million tons. The rocks of the basin are stratigraphically composed of two different units. The lower part is composed of Upper Jurassic (Oxfordian) to Lower Cretaceous (Aptian) volcanic-pyroclastic-epiclastic successions of up to 3500 m thick (Wang et al., 2002a). The upper part comprises a Lower Cretaceous (Albian) to Upper Cretaceous (Maastrichtian), sedimentary sequence of up to 5700 m thick (Wang et al., 1996). The volcanogenic successions are our main interest in this paper as they host the organic component for the oil.

Natural gases that are above cut-off grade for industry use include hydrocarbons, carbon dioxide and some noble gases like helium. The volume percent of the volcanic and sedimentary reservoirs is about half and half (50:50) in the studied area (Fig. 1). The volcanic rocks cover a wide spectrum from rhyolite to basaltic andesite with ages ranging from late Jurassic to early Cretaceous (Wang et al., 2002b). Typically the volcanic rocks are phenocryst-poor, with porphyritic texture and a complex phenocryst assemblage commonly including quartz, feldspars (sanidine, anorthoclase and plagioclase), biotite, magnetite and ilmenite. The phenocrysts are generally less than 20% in volume of the volcanic rocks and tuffs. Rock names and textures used in the paper follow the classifications of Le Maitre et al. (1989) and MacKenzie et al. (1982). Fluid inclusions seen in doubly polished wafers (200–300 μm in thickness) were carefully selected under the microscope; quartz crystals were selected, including from the rhyolite, dacite and andesite, which are the predominant volcanic rock reservoirs. For each sample we determined fluid inclusion compositions and homogenization temperature, conducted with microthermometry and Raman microspectroscopy (cf. Table 1) after having done thin-section, bulk, trace, and REE element analysis and isotopic dating (e.g. TAS, total alkali versus silica diagram, seen in

Table 2 Bulk natural gas components and isotopes hosted in the reservoir volcanic rocks corresponding to the fluid inclusion-bearing samples shown in Table 1

Well No.		FS9-2	FS9-1	ZS6	ShS2	SoS1	ZS5	SiS1	FS7
Depth (m)		3582	3697	3590	2907	3470	3529	3700	3710
Lithology		Volcanics	Volcanics	Volcanics	Tuff	Volcanics	Tuff	Tuff	Tuff
TAS		Rhyolite	Rhyolite	Rhyolite	Trachydacite	Trachyandesite	Rhyolite	Rhyolite	Rhyolite
Gas pool type		CH_4-bearing CO_2	CH_4-bearing CO_2	CO_2-bearing CH_4	CO_2-bearing CH_4	CO_2-bearing CH_4	CO_2-bearing CH_4	Mixture	Mixture
Production (m^3/day)		>40000	>1000	>100	>3×10⁵	>1000	>200	>20000	>40000
Gas component (mole%)	CH_4	15.1	10.9	90.5	81.6	96.4	93.4	37.9	57.4
	C_2^+	0.23	0.16	3.37	2.37	0.77	1.98	0.12	1.39
	$C_1/\Sigma C_1^+$	0.99	0.99	0.96	0.97	0.99	0.98	0.99	0.98
	CO_2	82.2	85.7	2.38	6.98	2.30	0.22	50.6	38.8
	He	2.44	2.74	0.06	0.01	0.02	0.03	n.d.	0.01
Isotope composition (‰) PDB	CH_4	−27.11	−27.25	−25.90	−28.71	−26.44	−25.90	−28.00	−29.52
	C_2H_6	−30.05	n.d.	−28.98	−28.95	−23.44	−28.98	−34.00	−30.72
	C_3H_8	−30.50	n.d.	−32.00	−35.01	−32.82	−32.00	−34.10	−29.90
	C_4H_{10}	−32.98	n.d.	n.d.	−37.58	−25.02	n.d.	n.d.	−27.83
	CO_2	−4.06	−5.46	n.d.	n.d.	n.d.	n.d.	n.d.	n.d.
$^3He/^4He$ ($\times10^{-6}$)		4.2	4.0	n.d.	n.d.	n.d.	n.d.	n.d.	n.d.

Note: (1) Gas samples were collected by Qijun Hou and analyzed at Daqing Institute of Exploration with mass spectrometry; (2) n.d. indicates not detected. Standard deviation for the carbon isotope analysis is from 0.5 to 0.8.

Table 1 of Wang et al., 2006).

As shown in Fig. 1, commercial reservoirs in the studied area can be classified into four groups according to a combination between reservoir rocks and gas geochemistry. They include: volcanic reservoirs, (a), hosting gases with heavy and reversed carbon isotopes; (b), hosting gases without heavy or reversed carbon isotopes; and sedimentary reservoirs, (c), hosting gases with heavy and reversed carbon isotopes; and (d), hosting gases without heavy or reversed carbon isotopes. We chose samples only from the first group for our study.

Up to now over 50 exploration wells have been drilled through these volcanic reservoirs. We selected eight of them for our study on the basis of their distribution, geology and gas-geochemistry (Dai et al., 1996). Drill cores of volcanic rocks and tuffs were collected from the eight representative gas reservoirs covering the three gas types of CO_2, CH_4 and CO_2-CH_4 mixtures (Table 2). In order to minimize the differences between samples arising from different ages and mineral evolution of the rocks, we chose quartz-bearing Lower Cretaceous (Barremian) rocks (Wang et al., 2002a) and, as noted above, used only quartz crystals for fluid inclusion measurements. Three types of fluid inclusions were recognized including secondary, primary and glassy ones. The latter two are of interest in this work.

3 Analytical Techniques

Microthermometry and Raman microspectroscopy were conducted at the Geofluid Laboratory of Jilin University with a British Renishaw System-1000 Laser Raman Spectrometer equipped with a Leica DMLM (objective ×50) microscope and a Linkam THMS-600 Heating-

Freezing Stage. Micro-Raman analytical conditions were as follows: Mark 514.532 nm Ar⁺ laser generator with a laser power of 20 mw, 1800 g/mm grating, slit width of 20 μm, scanning span 4500–850 cm^{-1}, integrated time 120 s. A charge coupled device (CCD) array detector was employed to detect the optical signal produced by the sample after analysis with an analytical precision of 1 cm^{-1}±. The spectrometer was calibrated with monocrystalline silica (520 cm^{-1}) before determination. The Heating-Freezing Stage was calibrated before microthermometric determinations at temperatures of −56.6ºC, 0ºC and 374.0ºC with man-made inclusions composed of 25% H_2O–75 mole% CO_2 and pure water. The analytical precision is 0.1ºC ± at low temperature (<30ºC) and 2ºC ± at high temperature.

The Micro-Raman quantitative data of the fluid inclusions were calculated with the Placzek's formula (Dhamelincourt et al., 1979). Raman intensity (integration area) was obtained using the specially designed Grams/32 software attached with the Renishaw System-1000 Laser Raman Spectrometer. The Raman cross-sections we used in our calculation for CO_2, CH_4 and N_2 contents are 1.21, 9.1 and 1.0, respectively. Based on laser Raman spectroscopic and microthermometric data of individual fluid inclusions, the bulk compositions were reconstructed with the method outlined in Ramboz et al. (1985) and are listed in Table 1. Any effect of salinity was ignored in the bulk fluid chemistry reconstruction because of the low salinity in the studied fluids. The critical parameter Z'_{CO_2} (Ramboz et al., 1985) used in our calculation was fixed at 2.0 mole% under the following considerations: (1) Micro-Raman spectrometric analysis at room temperature showed that the Raman peak of CH_4 was commonly at 2915 cm^{-1}± (2913 to 2917 cm^{-1}) equivalent to an inclusion internal pressure of
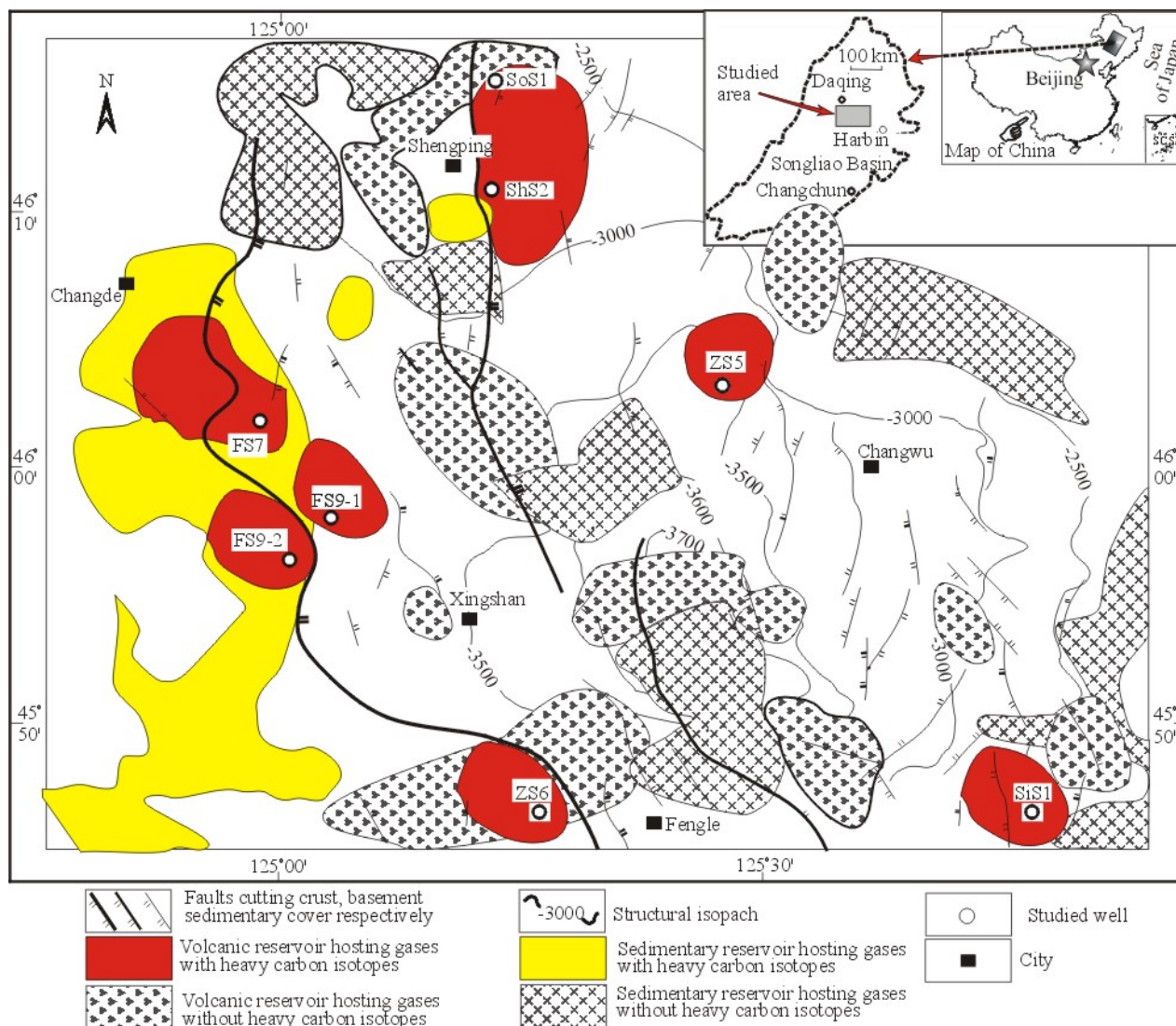
Fig. 1. Location and geological background of the studied wells in the central Songliao Basin, NE China, with a classification of commercial reservoirs.
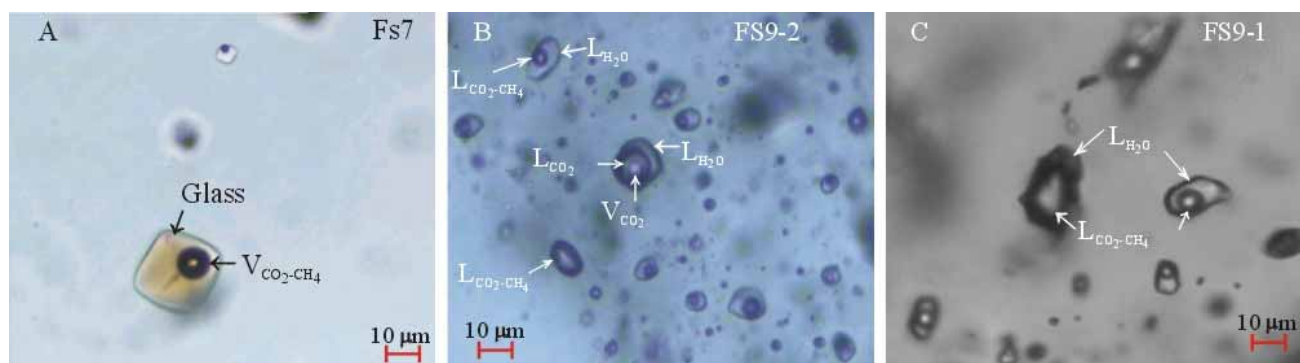

Fig. 2. Photographs of fluid inclusions from melt (A) and primary (B & C) sources in the reservoir volcanic rocks (rhyolite and dacite) of the Songliao Basin.

Sample numbers on the upper right correspond to those from Tables 1 and 2. V and L indicate phases of vapor and liquid.

ca. 100 bars according to Seitz et al. (1996) and, assuming an ideal mixture of real gases, the CO_2 solubility is about 1.06–2.2 mole% in low salinity water at the conditions of 10 MPa and from 0℃ to room temperature (according the experiment of Takenouchi and Kennedy, 1964); (2) Micro-Raman analysis for the liquid phase co-existing with a CH_4-CO_2 vapor showed that the dissolved CO_2 into the aqueous part of the inclusion is commonly in between 1.0–1.6
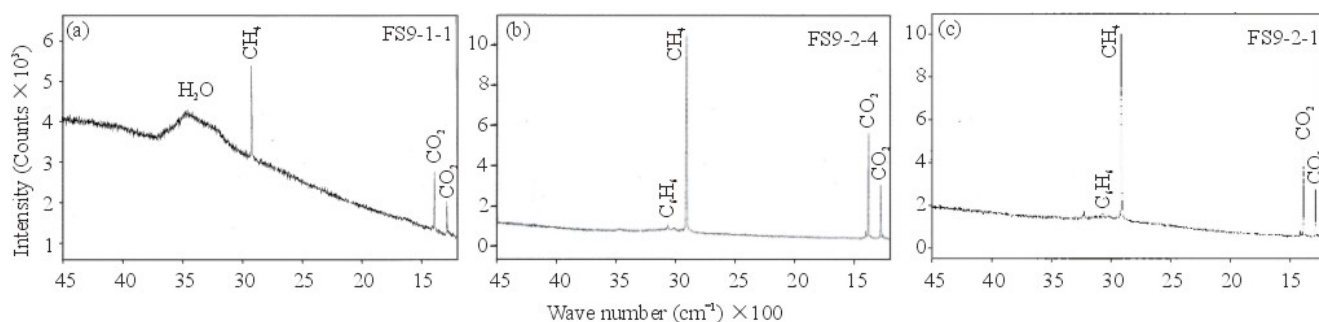
Fig. 3. Micro-Raman analyses of CH_4-CO_2-H_2O-bearing, vapor-dominated inclusions in the reservoir volcanic rocks of the Songliao Basin.

CH_4 in the samples is characterized by strong symmetric stretching lines at 2913–2917 cm^{-1}.

mole%.

4 Results and Discussions

4.1 Fluid inclusions

Fluid inclusions in matrix quartz or phenocryst/crystal quartz fragments are pervasive throughout the reservoir volcanic rocks. The inclusions occur both as secondary inclusions trapped along healed microfractures and as isolated or clustered primary inclusions that were trapped during mineral growth. Occasionally melts were trapped as glassy inclusions at high temperature (Fig. 2). In this study we focused on the latter two types of inclusions, especially the primary ones. Petrography, microthermometry and micro-Raman analysis indicate that quartz-hosted, CH_4-CO_2-H_2O-bearing fluid inclusions are the most common ones, followed by CH_4-CO_2 monophase inclusions. Triple phase inclusions filled with vapor-CO_2, liquid-CO_2 and liquid-H_2O can also be seen. Some inclusions contain a predominance of a CH_4-CO_2 phase (Fig. 3b, c), which can simply be considered as a CH_4-CO_2 binary system. For this reason we reconstructed only the CH_4, CO_2 and H_2O concentrations in fluid bulk compositions taken from Table 1. Although such minor components as CO, N_2, C_2H_2, C_6H_6, C_2H_4, H_2S and H_2 have been frequently detected in many inclusions we did not list them in Table 1 because their concentrations are generally only around detection limits.

For each sample we have analyzed several tens of fluid inclusions and most of them are aqueous ones that give Raman spectra of a strong stretching band of water (3000–3700 cm^{-1}) and a small symmetric stretching band of methane (2915±2 cm^{-1}) (Fig. 3a), which are similar to those described by Dubessy et al. (2001). High CH_4 fluid inclusions can occasionally be found. We selected one to five representative CH_4/CO_2-rich individual inclusions from each sample and list them here in Table 2. The size of the observed fluid inclusions ranged from 5 to 40 μm with a mode of 10–15 μm. Their non-aqueous part occupied 30%

to 100% of the cavity volume equivalent to degrees of filling of the inclusion ranging between 0.7 to 0.0 (i.e. *Flw*, Ramboz et al., 1985) and most of them ranged from 30% to 50% (*Flw* =0.7–0.5). Total homogenization temperature (*Th*) of the measured primary CH_4/CO_2-rich inclusions falls between 293–395ºC with a mode of 305–315ºC. The *Th* of the glassy inclusions is over 900ºC. Melting temperature of solid CO_2 in the presence of vapor (Tm_{CO2}) ranged from −56.9ºC to −69.2ºC with a mode around −61ºC to −64ºC. Homogenization temperature of the non-aqueous part to the liquid (Th_{CO2}) is between −45.2ºC and 8.6ºC. Melting temperature of clathrate (Tm_{Clath}) ranged from 8.1ºC to 14.8ºC. Salinity of the fluid inclusions shown in Table 1 was derived from Tm_{Clath} using the method of Ridley and Hagemann (1999) or using the formula of Collins (1979) when the CH_4 content was low. The salinities in our case studies are all around or below 5% in NaCl equivalent weight percent.

4.2 Relationship between fluid inclusions and commercial gases hosted in the same volcanic rocks

The relationship of the reconstructed bulk compositions between CH_4 and CO_2 in the volcanic fluid inclusions is shown in Fig. 4. The resulting curve is composed of three segments: (1) the CO_2-content of gases, which goes up rapidly with that of CH_4 in gas-poor inclusions; (2) the two components increase synchronously when CH_4 >10 mole% and CO_2> 30 mole%; (3) in gas-rich inclusions (more than 50 mole% CO_2 or CH_4), the CH_4-content correlates negatively with that of CO_2 with a slope about −1. This linear equation is nearly the same as that of bulk commercial gases hosted in the same volcanic reservoirs.

The former two cases seen in Fig. 4 relate to the fluid inclusions with relative high water content (79.3–88.4 mole%), in which concentrations of both CH_4 and CO_2 increase at the same time. Similar trends can be seen, as shown in Fig. 5, for the H_2O-CO_2-CH_4 system in primary inclusions hosted in ferberite from the carbonaceous and aqueous stage in quartz (Ramboz et al., 1985). For
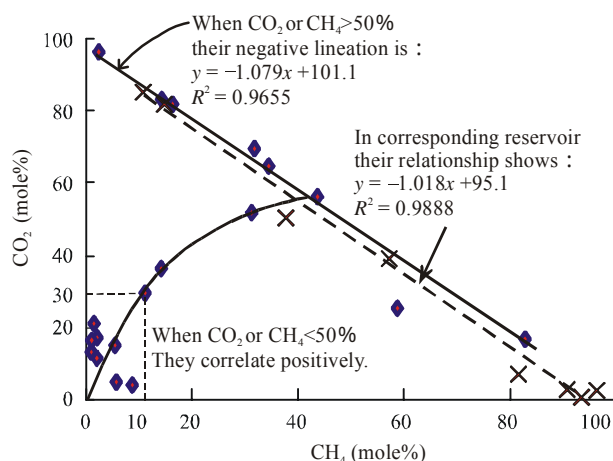
Fig. 4. Relationship of reconstructed bulk compositions between CO$_2$ and CH$_4$ in the primary inclusions of the volcanic rocks of the Songliao Basin (data from Table 1).
Dashed line and X indicate bulk gases in corresponding commercial reservoirs (data from Table 2).

Fig. 5. Relationship of reconstructed bulk compositions between CO$_2$ and CH$_4$ in the primary inclusions hosted in ferberite from the carbonaceous and aqueous stages in quartz (data from Ramboz et al., 1985, Tables 2 and 3).
Note that CO$_2$ and CH$_4$ have a positive correlation for all the three series showing a similar trend to those low-concentration gases hosted also in the quartz of the reservoir volcanic rocks of the Songliao Basin. Series1: inclusions with relatively high homogenization temperature (10.8–18.2°C) of non-aqueous part; Series 2: water (81.8–87.5%)-rich inclusions;Series3: inclusions with relatively high melting temperature (10.2–10.7°C) of clathrate.

comparison with the trapped gases in quartz we illustrate data of commercial gases trapped in the corresponding volcanic reservoirs (dashed line in Fig. 4). It is interesting to note that these commercial gases in the volcanic rocks also show strongly anti-correlated CH$_4$ and CO$_2$ (Fig. 4). This similarity tells us that CH$_4$ and CO$_2$ gases both from the fluid inclusions and from the reservoirs might have been regulated by similar processes. As we know that natural gas pools are fundamentally source-controlled, that is, a gas pool will mostly accumulate those gases with the most convenient migration path to the pool, we therefore interpreted those fluid inclusions with CH$_4$ or CO$_2$ more than 50% in mole as also source-controlled. There could be countless independent, inhomogeneously distributed sources of CH$_4$/CO$_2$ gases within the parent magma at the microscale, then the most convenient source of either CH$_4$ or CO$_2$ would contribute the most to the nearest inclusion and vice versa. This explanation can to some extent be proven by the inhomogeneous features of the fluid inclusions both in composition and distribution.

Trapped fluids in the volcanic rocks have a comparable composition to the content and isotopes of the gases from the same reservoirs. These affiliations can be attributed to their origin. The abiogenic hydrocarbons in the primary inclusions are initially mantle/magma derived. In addition, the inorganically derived gases, both CH$_4$ and CO$_2$, have contributed significantly to the corresponding gas pools. The results suggest that abiogenic methane can have industrial value and that the hydrocarbon budget of the bulk earth may be much larger than conventionally assumed.

4.3 Discussion

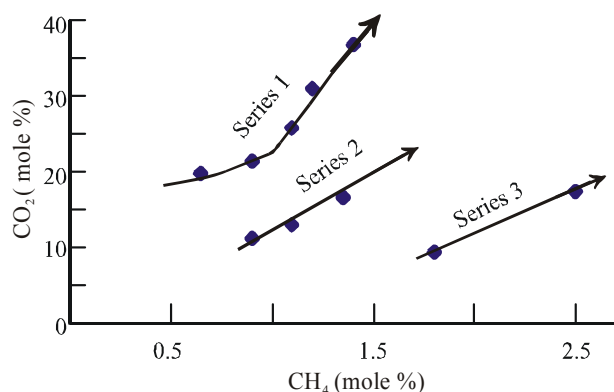The Cretaceous geothermal gradient of the studied area

is from 27°C/km to 44°C/km (Wang et al., 1993). The higher value can be used to interpret the melt inclusion (*Th* 900°C) hosted in the volcanic quartz because it correlates with the magmatic activities of the basin evolution (Wang et al., 1993). Accordingly, the quotient of 900°C/44°C·km^{-1} (ca. 20 km) can be considered as the maximum depth of inclusion formation because this would be the point of possible thermal equilibrium above which the magma might have been in complete thermal disequilibrium with the inclosing rocks during ascent. Taking into account that the Moho beneath the present Songliao Basin is at a depth of 30–35 km and that the boundary between the upper and lower crust is about 16 km (Yang et al., 2003), then a maximum closure depth of ca. 20 km suggests that the melt inclusions were formed at the lower crust depth or above.

The commercial gases hosted in CH$_4$-rich, fluid inclusion-bearing volcanic reservoirs (wells FS9-1 and FS9-2 in Table 2) show anomalous geochemical signatures with δ^{13}C values of CH$_4$ and CO$_2$ varying between −27.11 to −27.25‰, and −4.06 to −5.46‰, respectively, and an R/R_a ratio ranging from 2.88 to 3.02. These signatures are comparable to those of the fumarolic gases from Nisyros and Veuvio (Fiebig et al., 2004), where CO$_2$ and CH$_4$ were originally mantle-derived. On the other hand, some accessory minerals contained in the reservoir volcanic rocks, such as magnetite and ilmenite, are important geocatalysts in the abiogenic formation of hydrocarbons (Horita, 2001). Moreover, abiogenic methane can be generated by different kind of reactions, such as water-graphite and water-carbonate interactions either in the crust or in the earth's interior at different pressures and

temperatures (Glassley, 1982; Takach et al., 1987; Berndt et al., 1996; Scott et al., 2004). Fischer-Tropsch reactions among volatiles and minerals can also produce methane (Potter et al., 2004). Logically, the CO_2-rich fluid hosted in the melt inclusion (e.g. sample FS7) demonstrates that within or below the lower crust existed CO_2-rich fluids originating from mantle/magma outgassing. Then mineral reactions involving conversion of Fe^{II} to Fe^{II} occurred during magma ascent and led to production of H_2 and conversion of dissolved CO_2 to reduced-C species including methane, some of which were then trapped as CH_4-rich fluid inclusions. These multiphase mineral-mineral-fluid interactions must have happened under thermal disequilibrium as a whole or under micro-scale equilibrium resulting in intense heterogeneity of fluids enclosed in the volcanic minerals.

5 Conclusions

(1) Fluids blocked in the primary inclusions of the volcanic reservoir rocks are synchronous volatiles with the lava that was originally mantle/magma derived. The results of this study demonstrate that these volatiles can yield high amounts of methane. The co-existence and positive correlation between CO_2 and CH_4 in the primary inclusions suggest that they came from the same deep-seated sources. We can therefore conclude that the detected CH_4-containing primary inclusions in the reservoir volcanic rocks should be considered as direct evidence for inorganically derived natural gas.

(2) Concentration of CH_4 in the fluid inclusions goes up with increasingly heavy carbon isotopes and in reversed order of $\delta^{13}C$ in alkane, implying a strong influence on isotopes of the reservoir gases. That is to say, mantle/magma-derived abiogenic alkanes must have contributed significantly to the gas pools.

Acknowledgements

References

Berndt, M.E., Allen, D.E., and Seyfried, W.E. Jr., 1996. Reduction of CO_2 during serpentinization of olivine at 300°C and 500 bar. *Geology*, 24(4): 351–354.

Collins, P.L.F., 1979. Gas-hydrates in CO_2-bearing fluid inclusions and the use of freezing data estimation of salinity. *Econ. Geol.*, 74: 1435–1444.

Dai Jinxing, 1993. Characteristics of C and H isotopes and identification of different types of natural gases. *Natural Gas Earth Sciences*, (2/3): 1–40 (in Chinese with English abstract).

Dai Jin-xing, Song Yan, Dai Chun-sen and Wang Da-rui, 1996. Geochemistry and accumulation of carbon dioxide gases in China. *Bull. Am. Assoc. Petroleum Geol.*, 80(10): 1615–1626.

Dai Jinxing, Xia Xinyu, Qin Shengfei and Zhao Jingdan, 2003. Causation of partly reversed orders of biogenic alkane gas in China. *Oil & Gas Geology*, 24(1): 1–11 (in Chinese with English abstract).

Dhamelincourt, P., Beny, J. M., and Dubessy, J., 1979. Analyse d'inclusions fluides à la microsonde MOLE à l'effect Raman. *Bull. Mineral.,* 102: 600–610 (in French).

Dubessy, J., Buschaert, S., Lamb, W., and Pironon, J., 2001. Methane-bearing aqueous fluid inclusions: Raman analysis, thermodynamic modeling and application to petroleum basins. *Chem. Geol.*, 173: 193–205.

Fiebig, J., Chiodini, G., Caliro, S., Rizzo, A., Spangenberg, J., and Hunziker, J.C., 2004. Chemical and isotopic equilibrium between CO_2 and CH_4 in fumarolic gas discharges: generation of CH_4 in arc magmatic-hydrothermal systems. *Geochim. Cosmochim. Acta*, 68(10): 2321–2334.

Glassley, W., 1982. Fluid evolution and graphite genesis in the deep continental crust. *Nature*, 295(21): 229–231.

Guo Zhanqian and Wang Xianbin, 1994. Abiotic origin gas in Songliao Basin. *Sci. China* (B), 24(3): 303–309 (in Chinese).

Guo Zhanqian, Wang Xianbin and Liu Wenlong, 1997. Reservoir-forming features of abiotic origin gas in Songliao Basin. *Sci. China* (D), 40(6): 621–626.

Horita, J., 2001. Carbon isotope exchange in the system CO_2-CH_4 at elevated temperatures. *Geochim. Cosmochim. Acta*, 65(12): 1907–1919.

Huang Haiping, 2000. Isotopic reversal in natural gas: an example of deep strata gases from Xujianweizi depression, Songliao Basin. *Earth Sci.—J. China Univ. Geosci.,* 25(6): 617–623 (in Chinese with English abstract).

Kelley, D.S., 1996. Methane-rich fluids in the oceanic crust. *J. Geophys. Res.*, 101(B2): 2943–2962.

Le Maitre, R.W., Bateman, P, Dudek, A., Keller, J., Lameyre, M. J., Lebas, M.J., Sabine, P.A., Schmid, R., Sorensen, H., Streckeisen, A., Wooley, A.R., and Zanettin, B., 1989. *A Classification of Igneous Rocks and Glossary of Terms.* London: Blackwell, 193.

Li Chunyuan, Wang Xianbin and Xia Xinyu, 1999. The possibility and explanation of complete reverse isotopic distribution of light hydrocarbon in natural gas. *Acta Sedimentologica Sinica*, 17(2): 306–311 (in Chinese with English abstract).

Liu Gang, Wang Xianbin and Wen Qibin, 1998. Carbon isotopes of mantle-derived inclusions in the alkali-basalt of Zhangjiakou, NE China. *Chinese Sci. Bull.*, 41(19): 2098–2101 (in Chinese).

MacKenzie, W. S., Donaldson, C. H., and Guilford, C., 1982. *Atlas of Igneous Rocks and Their Textures*. London: Longman

Group Limited, 99.

Potter, J., Rankin, A. H., and Treloar, P. J., 2004. Abiogenic Fischer-Tropsch synthesis of hydrocarbons in alkaline igneous rocks; fluid inclusion, textural and isotopic evidence from the Lovozero complex, N.W. Russia. *Lithos*, 75: 311–330.

Ramboz, C., Schnapper, D., and Dubessy, J., 1985. The *P-V-T-X-fO₂* evolution of H$_2$O-CO$_2$-CH$_4$- bearing fluid in a wolframite vein: reconstruction from fluid inclusion studies. *Geochim. Cosmochim. Acta*, 49: 205–219.

Ridley, J., and Hagemann, S.G., 1999. Interpretation of post-entrapment fluid-inclusion re-equilibration at the Three Mile Hill, Marvel Loch and Griffins Find high-temperature lode-gold deposits, Yilgarn Craton, Western Australia. *Chem. Geol.*, 154: 257–278.

Sakata, S., Takahashi, M., Igari, S.I., and Noriyuki, S., 1989. Origin of light hydrocarbons from volcanic rocks in the "Green Tuff" region of northeast Japan: biogenic versus magmatic. *Chem. Geol.*, 74: 241–248.

Salvi, S., and Williams-Jones, A. E., 1997. Fischer-Tropsch synthesis of hydrocarbons during sub-solidus alteration of the Strange Lake peralkaline granite, Quebec/Labrador, Canada. *Geochim. Cosmochim. Acta*, 61(1): 83–99.

Scott, H.P., Hemley, R.J., and Mao, H.K., 2004. Generation of methane in the Earth's mantle: In situ high pressure-temperature measurements of carbonate reduction. *Proc. Nat. Acad. Sci. USA*, 101(39): 14023–14026.

Seitz, J.C., Pasteris, J.S., and Chou, I.M., 1996. Raman spectroscopic characterization of gas mixtures II: quantitative composition and pressure determination of the CO$_2$-CH$_4$ system. *Am. J. Sci.*, 296: 577–600.

Sheppard, S.M.F., 1981. Stable isotope geochemistry of fluids. *Phys. Chem. Earth*, 13/14: 419–443.

Takach, N.E., Barker, C., and Kemp, M.K., 1987. Stability of natural gas in the deep subsurface: thermodynamic calculation of equilibrium compositions. *Bull. Am. Ass. Petroleum Geol.*, 71(3): 322–333.

Takenouchi, S., and Kennedy, G.C., 1964. The solubility of carbon dioxide in NaCl solutions at high temperatures and pressures. *Am. J. Sci.*, 263: 445–454.

Wakita, H., and Sano, Y., 1983. ³He/⁴He ratios in CH$_4$-rich natural gases suggest magmatic origin. *Nature*, 305: 792–794.

Wang Pu-Jun, Chen Fukun, Chen Shu-Min, Siebel, W., and Muharrem, S., 2006. Geochemical and Nd-Sr-Pb isotopic composition of Mesozoic volcanic rocks in the Songliao basin, NE China. *Geochem. J.*, 40: 149–159.

Wang Pujun, Du Xiaodi, Wang Jun and Wang Dongpo, 1996. Chronostratigraphy and stratigraphic classification of the Cretaceous of the Songliao Basin. *Acta Geologica Sinina* (English edition), 9(2): 207–217.

Wang, P.J., Liu, W.Z., Wang, S.X., and Song, W.H., 2002a. ⁴⁰Ar/³⁹Ar and K/Ar dating on the volcanic rocks in the Songliao basin, NE China: constraints on stratigraphy and basin dynamics. *Geologisches Rundschau*, 91: 331–340.

Wang, P.J., Ren, Y.G., Shan, X.L., Sun, S.B., Wan, C.B., and Bian, W.H., 2002b. The Cretaceous volcanic succession around the Songliao Basin, NE China: relationship between volcanism and sedimentation. *Geol. J.*, 37(2): 97–115.

Wang Tieguan, Zhu Dan, Lu Hong, Zhang Zhihuan and Yang Chiyin, 2004. Biodegraded oil and its high molecular weight (C$_{35+}$) n-alkanes in the Qianmiqiao Region in Bohai Basin, Northern China. *Acta Geologica Sinica* (English edition), 78 (4): 993–1001.

Wang Xianbin, Wu Maobin and Zhang Mingjie, 2000. Stable isotope geochemistry of mantle fluids. *Geology & Geochemistry*, 28(3): 69–74 (in Chinese with English abstract).

Wang Zhiwu, Yang Jiliang and Gao Ruiqi, 1993. *Petroleum Geology of China Vol. 2: Daqing Oil Field*. Beijing: Petroleum Industry Press, 785 (in Chinese).

Xu Sheng, Nakai S'i., Wakita, H., and Wang Xianbin, 1995. Mantle-derived noble gases in natural gases from Songliao basin, China. *Geochim. Cosmochim. Acta*, 59(22); 4675–4683.

Yang Baojun, Tang Jianren, Li Qinxue, Wang Jianmin, Faisal, S. A., Li Ruilei, Wang Hongzhi, Li Zhanlin and Zhang Hui, 2003. Seismic reflection structure and "discontinuity" of Moho beneath the Songliao Basin. *Sci. China* (D), 33(2): 170–176 (in Chinese).

Zheng Jianjing, Ji Liming and Meng Qianxiang, 1999. Thermal simulation research of partial opposites sequence of carbon isotope and ethane carbon isotope of gases. *Acta Sedimentologica Sinica*, 17(Supp.): 811–814 (in Chinese with English abstract).